Carbohydrate Polymers 92 (2013) 1737–1742

Contents lists available at SciVerse ScienceDirect

Carbohydrate Polymers

journal homepage: www.elsevier.com/locate/carbpol

The crystal structure of mono-ethylenediamine β-chitin from synchrotron X-ray fiber diffraction

Daisuke Sawada[a,*], Satoshi Kimura[a,b], Yoshiharu Nishiyama[c], Paul Langan[d], Masahisa Wada[a,b]

[a] Department of Biomaterial Sciences, Graduate School of Agricultural and Life Sciences, The University of Tokyo, 1-1-1, Yayoi, Bunkyo-ku, Tokyo, Japan
[b] Department of Plant & Environmental New Resources, College of Life Sciences, Kyung Hee University, 1, Seocheon-dong, Giheung-ku, Yongin-si, Gyeonggi-do 446-701, Republic of Korea
[c] Centre de Recherches sur les Macromolécules Végétales (CERMAV-CNRS), BP 53, F-38041 Grenoble Cedex 9, France
[d] Biology and Soft Matter Division, Oak Ridge National Laboratory, Oak Ridge, TN 37831, USA

ARTICLE INFO

Article history:
Received 19 July 2012
Received in revised form 6 November 2012
Accepted 7 November 2012
Available online 17 November 2012

Keywords:
β-chitin
Crystal structure
X-ray fiber diffraction
Ethylendiamine
GlcNAc
Intercalation

ABSTRACT

The crystal structure of a complex of β-chitin with ethylenediamine (EDA) was determined by synchrotron X-ray fiber diffraction. Data were collected from a sample prepared from the bathophilous tubeworm *Lamellibrachia satsuma*. The unit cell contains one chain having one *N*-acetylglucosamine residue in the asymmetric unit with the hydroxymethyl group in *gt* conformation ($a = 4.682$ Å, $b = 14.351$ Å, $c = 10.275$ Å and $\gamma = 96.24^\circ$ in space group $P2_1$). The complexed EDA molecule has a trans conformation with one amino group tightly bound to the primary alcohol hydroxyl group O6 atom of the *N*-acetylglucosamine residue in an arrangement similar to that found in the EDA–cellulose I complex. The other amino group has no detectible hydrogen bonding and higher thermal displacement. This common interaction between EDA and O6 would appear to be the dominant driving interaction for complex formation with both β-chitin and cellulose.

1. Introduction

Chitin is composed of β-1,4 linked 2-acetamido-2-deoxy-D-glucan that is often embedded in protein and is found partly deacetylated after purification process. A few studies suggest a covalent cross-linking between protein and chitin to be responsible for the high mechanical strength of insect cuticles or squid beaks (Kerwin, Whitney, & Sheikh, 1999; Miserez, Li, Waite, & Zok, 2007; Miserez, Rubin, & Waite, 2010; Schaefer et al., 1987). Chitin–protein complexes play a structural role in the protective shells of arthropods (Muzzarelli, 2011) and vestimentiferan tube worms similar to that played by lignocellulose composites in plant cell walls. Despite their potential as abundant and renewable resources, both cellulose and chitin are insoluble in common solvents, making the application of standard industrial processing difficult. Many known solvents of chitin, such as dimethylacetamide with salts (Austin, Brine, Castle, & Zikakis, 1981) are common to cellulose. Thus crystal structures of chitin with coordinated solvents can also provide information relevant to the interaction of cellulose with small molecules.

Two major naturally occurring crystal allomorphs of chitin, namely α-chitin and β-chitin, have been identified from their distinct X-ray diffraction patterns, infrared spectra and NMR spectra (Blackwell, 1973; Rudall, 1963; Tanner, Chanzy, Vincendon, Roux, & Gaill, 1990). β-chitin can incorporate various small molecules (Blackwell, 1969; Noishiki, Nishiyama, Wada, Okada, & Kuga, 2003; Noishiki, Kuga, Wada, Hori, & Nishiyama, 2004; Saito, Okano, Gaill, Chanzy, & Putaux, 2000; Yoshifuji, Noishiki, Wada, Heux, & Kuga, 2006) to form crystalline complexes (crystallosolvates) of which the most important and thoroughly studied are the hydrates (Blackwell, 1969; Gaill, Persson, Sugiyama, Vuong, & Chanzy, 1992; Kobayashi, Kimura, Togawa, & Wada, 2010; Rössle et al., 2003; Saito, Kumagai, Wada, & Kuga, 2002; Tanner et al., 1990). Recently, we determined the anhydrous and dihydrate structures of β-chitin using synchrotron X-ray and neutron fiber diffraction (Nishiyama, Noishiki, & Wada, 2011; Sawada et al., 2012a, 2012b). The arrangement of the molecules in the *a*-axis direction and the molecular geometry of the backbone were similar in the anhydrous and dihydrate forms, although the acetamide group was more relaxed in the dihydrate form. On the other hand, the hydrogen bonding system was drastically different in the two forms, with only the hydrogen bonding between amide groups being common. In particular, the intramolecular hydrogen bond between hydroxyl

* Corresponding author at: Department of Biomaterials Science, Graduate School of Agricultural and Life Sciences, The University of Tokyo, 1-1-1, Yayoi, Bunkyo-ku, Tokyo 113-8657, Japan. Tel.: +81 3 5841 5247; fax: +81 3 5841 2677.
E-mail addresses: utkspecial@hotmail.com, dsawada.ut.bm@gmail.com (D. Sawada).

0144-8617/$ – see front matter © 2012 Elsevier Ltd. All rights reserved.
http://dx.doi.org/10.1016/j.carbpol.2012.11.025

O3 and ring oxygen O5 was absent in the dihydrate structure and most hydrogen bonding involved the guest water molecules. Such detailed structural information has only recently become available through the development of high-resolution fiber diffraction analysis technologies with synchrotron X-ray and neutrons sources over the past decade.

Amines are known to penetrate cellulose and chitin crystals, and constitute classic solvents of cellulose combined with heavy metals such as copper. When used in a pure form, amines form crystallosolvates with cellulose and chitin, including α-chitin(Noishiki, Nishiyama, Wada, & Kuga, 2005) which does not allow water penetration into the crystal. Ethylenediamine (EDA) has been one of the most important reagents for studying these interactions because it is liquid at ambient conditions and relatively easy to handle. The detailed crystal structure(Wada, Heux, Nishiyama, & Langan, 2009) and the stability(Wada, Kwon, & Nishiyama, 2008) of EDA–cellulose I and the structure of an ammonia–cellulose I complex have been reported recently. For β-chitin, Noishiki and coworkers reported two types of EDA complex which differ in their guest–host ratio, namely Type I and Type II. In Type I there is one EDA molecule per two GlcNAc residues (hemi-EDA complex) and in Type II there is one per one GlcNAc residue (mono-EDA complex) (Noishiki et al., 2003). Both the EDA cellulose I complex and the mono-EDA complex correspond to a non-staggered one-chain monoclinic unit cell with one EDA molecule per residue. In this study, we report the detailed crystal structure of mono-EDA determined using synchrotron X-ray diffraction, and we compare the molecular interactions with those in cellulose–amine complexes.

2. Experimental

2.1. Sample preparation

Satsuma tubeworms (*Lamellibrachia satsuma*) were collected from the sea off Kagoshima Bay at a depth of about 100 m using a remotely operated vehicle, Hyper-Dolphin (JAMSTEC, Japan). The samples were purified and oriented as described previously (Kobayashi et al., 2010; Ogawa, Kimura, & Wada, 2011).

2.2. Data collection

Synchrotron X-ray fiber diffraction data were collected at beamline BL40B2 at SPring-8 (Hyogo, Japan). The oriented fibers were inserted into a glass capillary and immersed in EDA. The capillary was then sealed by flame and mounted perpendicular to the beam (λ = 0.7 Å) on a goniometer. A fiber diffraction pattern was recorded using a flat imaging plate (IP) (R-AXIS IV++, Rigaku) with an exposure time of 180 s. The sample-to-IP distance, about 196 mm, was calibrated using Si powder (d = 0.31355 nm) (Sikorski, Hori, & Wada, 2009).

In the X-ray fiber diffraction pattern, Fig. 1, there are noticeable diffraction peaks in the meridian direction corresponding to (0 0 1) and (0 0 3) reflections, but their relative intensities are small (∼1% of the intensity of the (0 0 2) reflection). Therefore the space group symmetry was approximated as $P2_1$. D-spacings of 20 reflections were measured using R-axis software, indexed with a monoclinic unit cell, and then used for least squares refinement of the unit cell parameters (d-spacing values are listed in Table S1); a = 4.682 Å, b = 14.351 Å, c = 10.275 Å, and γ = 96.24°.

A polarization correction (with a linear coefficient of 0.83), background subtraction, and peak fitting were carried out as described previously (Nishiyama et al., 2011). The diffraction pattern was transformed to a polar-coordinate intensity matrix of 360 by 2000 elements, corresponding to 1° increment in azimuthal angle and a 100-micron interval in reciprocal polar radius. The background

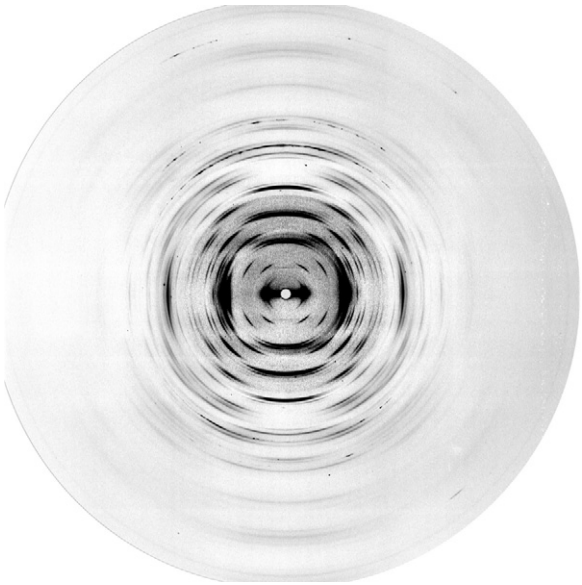

Fig. 1. The raw X-ray diffraction pattern of mono-EDA β-chitin complex. The fiber direction (meridian) is vertical and the equator is horizontal.

was evaluated for each radial trace using a bicubic spline function with a grid point every 50 pixels. Fig. S1 shows the observed (A) and fitted (B) diffraction data in polar coordinates. The fitted intensity of each Miller index (individual reflection) was kept in a "crude intensity list" for calculation of Fourier syntheses. However for structure refinement we grouped neighboring reflections on the same layer line that were close enough to overlap (because of cylindrical averaging) into composite intensities in a "regrouped intensity list".

2.3. Structure solution

X-ray structure refinement was carried out using previously described strategies for applying SHELX-97 (Sheldrick, 1997) to fiber diffraction data (Langan, Nishiyama, & Chanzy, 2001). The backbone of the recently reported atomic resolution structure of anhydrous β-chitin (Nishiyama et al., 2011) was taken as the phasing model. Bond lengths and bond angles were restrained to the average values of the β-(1–4)-*N*-acetyl-D-glucosamine dimer trihydrate (Mo, 1979) using the DFIX and DANG options in SHELX-97 with default standard deviations. An initial refinement was carried out with the hydroxymethyl group O6 removed and using the crude intensity list up to 1.47 Å resolution (atomic numbers were shown in Fig. 4c). The meridional intensities were also omitted. Both positional parameters and individual isotropic atomic displacement parameters were refined. This involved 136 amplitudes with $Fo > 4\sigma(Fo)$, 43 parameters, with 71 restraints. Two distinct structures corresponding to the chains pointing either up or down in the unit cell were refined, as defined by French and Howley (1989).

Both Fo–Fc and 2mFo–Fc (σ_A) omit maps were calculated and then visualized by using *Coot* (Emsley & Cowtan, 2004) and *Raster3D* (Merritt & Bacon, 1997, p. 3) software. Refinement of the "down" model resulted in a value of 0.3457 for R1, (R1 is calculated from $\sum(|Fo| - |Fc|)/\sum|Fo|$ with $Fo > 4\sigma$, where Fo and Fc are the observed and calculated amplitudes, respectively) and there were clear density peaks present in the resulting Fo–Fc map (Fig. 2b) that could be associated with possible positions for the omitted O6 atom of the hydroxymethyl group and the two C atoms of the EDA molecule. Refinement of the "up" model resulted in a value of 0.4338 for R1, and density peaks were not found that could be associated

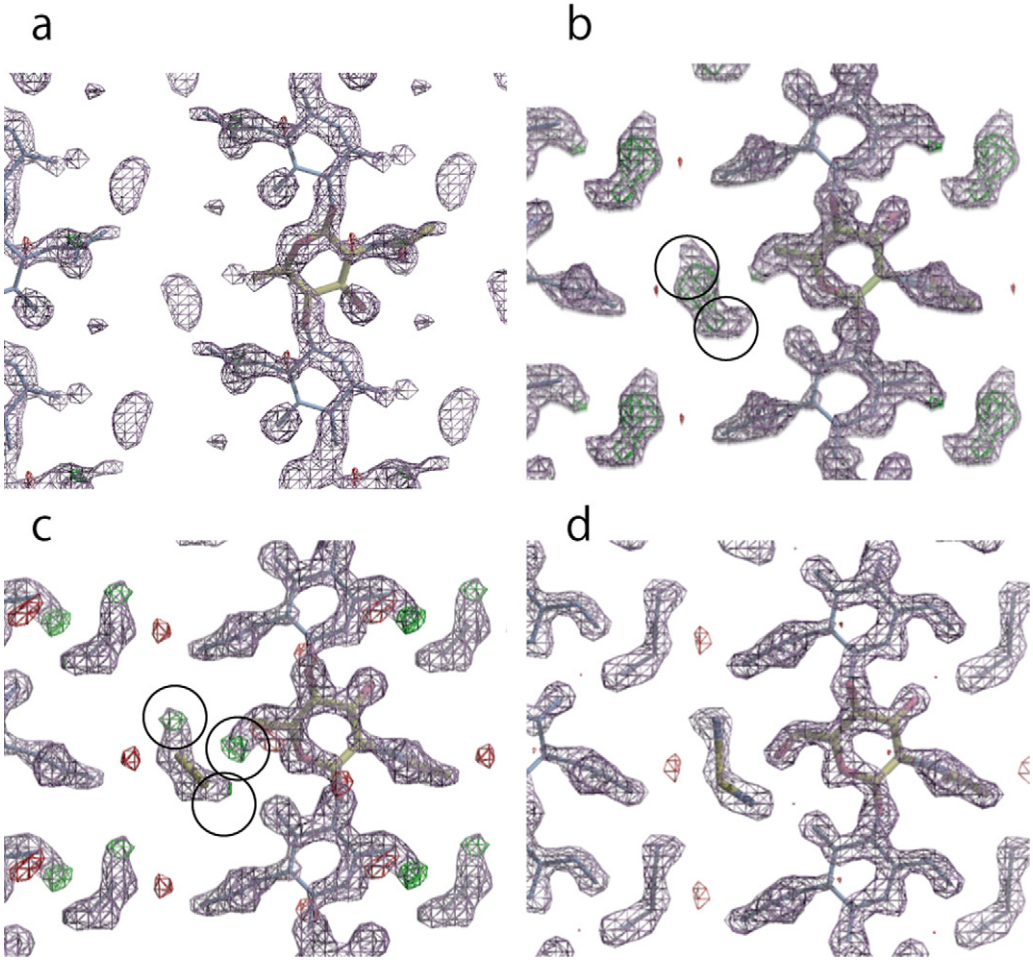

Fig. 2. Section through the X-ray σ_A map (showing positive density in blue) and the X-ray Fo–Fc omit map (showing positive and negative density in green and red, respectively). (a) Calculated using only the backbone (omitting O6) with parallel-up configuration as phasing model. (b) Parallel-down. Density indicated by circles can be associated with the EDA C11 and C12. (c) Calculated after introduction of C11 and C12. Density indicated by circles can be associated with the two nitrogen atoms of EDA labeled N11, N12 and hydroxymethyl O6. (d) Calculated with the complete molecular model (excluding hydrogen). (For interpretation of the references to color in this figure legend, the reader is referred to the web version of the article.)

with the omitted atoms in the corresponding omit maps (Fig. 2a). Thus the "up" model was discarded. The omitted atoms were then sequentially introduced at the positions of residual electron density peaks. Subsequent refinements were carried out with bond angle and bond distance restraints applied to the additional atoms. The C—C and C—N bond lengths were restrained to 1.545 and 1.469, and C—C—N bond angle was restrained by the 1–3 distance of 2.5 Å (Yokozeki & Kuchitsu, 1971). The sequential addition of C11 and C12 (Fig. 2c), O6, and finally N11 and N12 (Fig. 2d) resulted in values of 0.2834, 0.2613, and 0.2359 for R1, respectively.

Further refinement was carried out using the regrouped intensity list, resulting in a reduction in the number of data (Fo > 4σ(Fo)) to 77, and a value of 0.1424 for R1. Incorporation of hydrogen atoms attached to carbon and acetamide nitrogen atoms at standard positions using the HFIX option resulted in a value of 0.1417 for R1. A refinement with isotropic atomic displacement parameters restrained with the SIMU option gave a value 0.1245 for R1. Finally intensities, whose relative structure factor Fc/Fcmax was smaller than 0.085, were omitted using previously described strategies (Fig. S2) (Langan et al., 2001), reducing the number of reflections to 72. This resulted in small changes in atom positions of the EDA molecule and a value of 0.1108 for R1 after refinement. The coordinates of the final X-ray structure are available as a crystallographic information file (cif) file in the supplementary information.

3. Results and discussion

3.1. Structure

The unit cell parameters for the EDA β-chitin complex determined in this study, $a = 4.682$ Å, $b = 14.351$ Å, $c = 10.275$ Å, $\gamma = 96.24°$, are similar to those previously reported, $a = 4.79$ Å, $b = 14.50$ Å, $c = 10.37$ Å, $\gamma = 96.7°$ (Noishiki et al., 2003). The chains have a parallel-down packing arrangement, as does dihydrate β-chitin, (Sawada et al., 2012b) whereas anhydrous β-chitin (Nishiyama et al., 2011; Sawada et al., 2012a) has a parallel-up arrangement. This conversion between the "up" and "down" descriptions of the chain arrangement just corresponds to a change in the definition of the γ angle, due to small changes in the spacing between the stacked sheets and not to a physical change in chain direction (Fig. 3).

Based on the unit cell volume of anhydrous β-chitin (459.4 Å^3) and the bulk density of EDA (0.899 g/cm^3) we would expect that a complex containing one EDA molecule per GlcNAc residue would have a unit cell volume of 681.4 Å^3. This is slightly smaller than the experimentally derived value for mono-EDA β-chitin (686.30 Å^3) and suggests a higher free volume after complexation. Dihydrate β-chitin and EDA–cellulose I have smaller free volumes which can be estimated from bulk densities.

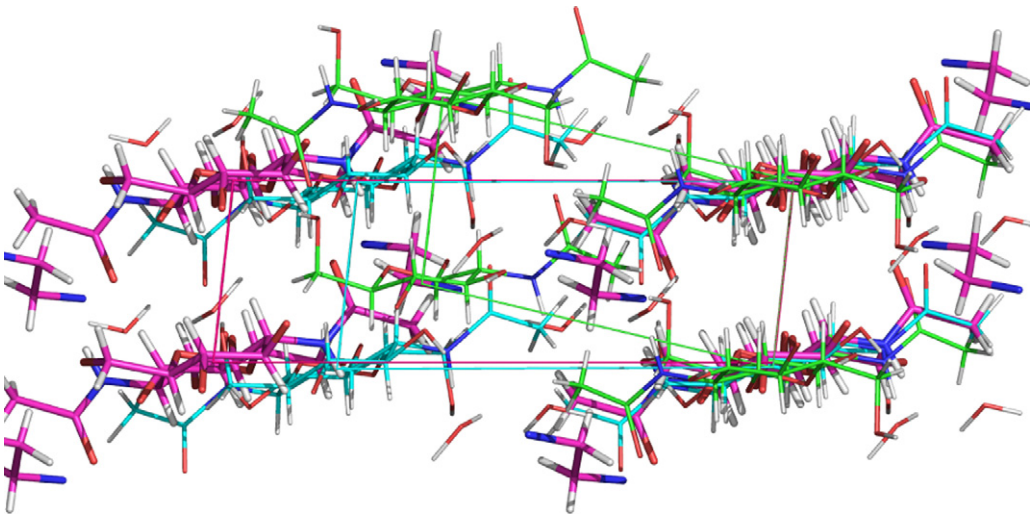

Fig. 3. Superposition seen from the non-reducing end of mono-EDA β-chitin (purple backbone and cell), dihydrate (cyan), and anhydrous structure (green). (For interpretation of the references to color in this figure legend, the reader is referred to the web version of the article.)

The Fourier difference maps indicate that there is one EDA molecule per GlcNAc residue, which is in agreement with the experimental evaluation using thermogravimetry and the size of unit cell. When the crystallographic refinement was carried out allowing the occupancy of EDA to refine, it refined to a value of 1.07. There was no significant change in the value of R1 (0.1079) during this refinement indicating that a value of unity is in good agreement with the data. The isotropic thermal displacement parameters of EDA were much larger than the chitin molecule (Fig. 4c). The isotropic thermal displacement parameters of the four EDA atoms, N12, C12, C11 and N11 were 0.3613, 0.3834, 0.3766 and 0.4430, respectively. The N12 atom, which is linked to the chitin molecule by a hydrogen bond, is more localized than the N11 atom, which does not participate in strong hydrogen bonding.

3.2. Hydrogen bonding

Relaxed geometric criteria were used in identifying the potential hydrogen bonds listed in Table 1 and represented in Fig. 4; a distance range between donor and acceptor of >2.4 Å and <3.7 Å was used. According to these criteria, O3 can donate a hydrogen atom in potential hydrogen bonds to O6, O5, or N12, with a bifurcated hydrogen bond to O5 and O6 being most favorable. The nitrogen N12 atom can participate in several hydrogen bonds of varying strengths whereas the N11 and C11 atoms can participate only in a few weak hydrogen bonds. In particular, O6 can donate a hydrogen atom to N12 ($x-1$, y, z) in very favorable hydrogen bonding geometry. Amines, such as ammonia, are known to be better hydrogen bond accepters than donors, and it is possible that a strong O6—H. . .N12 hydrogen bond might be the main driving force leading to the intracrystalline penetration of EDA and the conformational change of O6 from *gg* to *gt*.

Table 1
Potential hydrogen bonds.

Donor	Acceptor	Do. . .A distance (Å)	R—Do. . .A(°)	Acceptor residue
N2	O7	2.71	–	$x+1,y,z$
O3	O5	2.90	92	$-x,-y,1/2+z$
O3	O6	3.14	120	$-x,-y,1/2+z$
O3	N12	3.42	160	$-x,-y,1/2+z$
O6	O5	2.39	70	x,y,z
O6	O3	3.14	124	$-x,-y,-1/2+z$
O6	N12	2.54	139	$x-1,y,z$
O6	N12	3.67	121	x,y,z
N12	O6	2.54	99	$x+1,y,z$
N12	O6	3.67	86	x,y,z
N12	O3	3.42	137	$-x,-y,-1/2+z$
C11	O6	3.04	–	x,y,z
C2	O7	2.85	–	x,y,z
C8	N11	3.23	–	$-x,-y,-1/2+z$
C8	N11	3.59	–	$x,y+1,z$

Do, donor; A, acceptor.

Alternating strong hydrogen bonds between N12 and O6 along the hydrophobic stacks of chains form a homodromic cooperative chain of hydrogen bonds. This type of cooperative hydrogen bonding has been observed before in cellulose III_I (Parthasarathi et al., 2011; Wada, Chanzy, Nishiyama, & Langan, 2004), dihydrate β-chitin (Sawada et al., 2012b), and EDA–cellulose I. Interestingly, in the case of EDA–cellulose I and EDA–β-chitin the same O6 and N12 atoms are involved. This hydrogen bonding network can form in two opposite directions along the *a*-axis. The R—Do. . .A hydrogen bond angles of (99°, 121°) and (139°, 86°) indicate that the former case (Fig. 4a) results in more linear hydrogen bonds. On the other hand, in the latter case (Fig. 4b) the accepting capability of nitrogen atom is stronger than donating, i.e. N12 accepting hydrogen bond length becomes 2.54 Å. The latter case has another advantage because the O3 could accept the hydrogen bond from N12. Neutron diffraction will be required to directly locate hydrogen atoms in EDA–cellulose I and EDA–β-chitin in order to experimentally differentiate between these two possible arrangements.

Mono-EDA–β-chitin converts to the hemi-EDA complex under vacuum dried conditions (Noishiki et al., 2003). Although the crystallographic unit cell of the hemi-EDA complex has not been determined yet, Noishiki et al. investigated the thermal conversion from mono-EDA to hemi-EDA using X-ray diffraction. In those studies the mono-EDA peaks completely disappeared at temperatures above 160 °C and the hemi-EDA peaks disappeared at temperature above 280 °C. One explanation for the less of EDA from the mono-EDA β-chitin complex is the relative small number of potential hydrogen bonds observed in this study. Furthermore the loss of EDA from mono-EDA β-chitin and EDA–cellulose I occurs at almost the same temperature, suggesting that the EDA molecules might have similar energy barriers regardless the hydrogen bonding number.

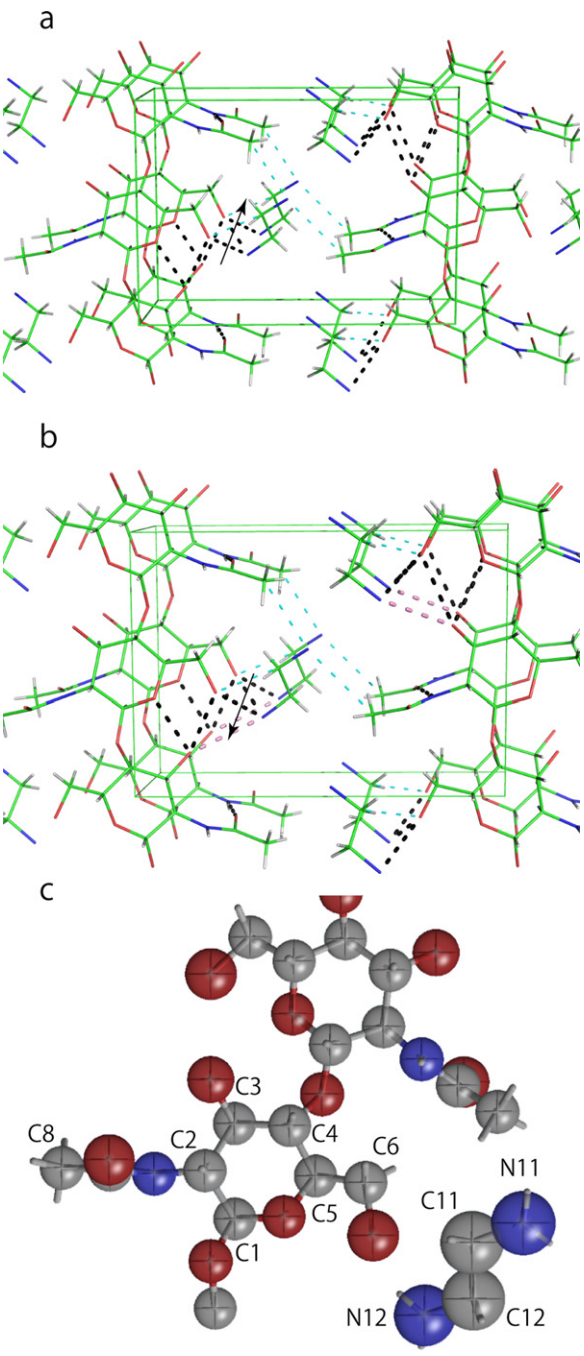

Fig. 4. The hydrogen bonding models of EDA β-chitin complex. Weak hydrogen bonds were shown by blue dash. Pink dash hydrogen bonds were appeared in the case of b. The direction of consecutive hydrogen bond was shown by arrow mark. ORTEP representation at 20% probability level (c). (For interpretation of the references to color in this figure legend, the reader is referred to the web version of the article.)

3.3. Conformational parameters

Major conformational parameters of EDA β-chitin complex are listed in Table 2. Interestingly, the torsion angle C4—C5—C6—O6 (ω') of 153° corresponds to the *gt* conformation, and not the *gg* conformation found in anhydrous and dihydrate β-chitin. The *gt* conformation is found in most cellulosic crystals including the EDA–cellulose I complex (Wada et al., 2009). The deviation of 27° from the ideal dihedral angle is probably due to the hydrogen bond with EDA with some contribution of hydrogen bonding from O3.

Table 2
Conformational parameters of EDA β-chitin complex.

	τ	ω	ω'	ϕ	ψ	θ
This structure	115 (3)	32 (6)	153 (5)	−95 (4)	−144 (3)	10 (7)
dihydrate	115	−54	67	−95	−147	6.6
Anhydride	117	−65	58	−89	−152	10

τ: Glycosidic bond angle, torsion angles; ω: O5C5C6O6, ω': C4C5C6O6, ϕ: O5C1O1C4', ψ: C1O1C4'C5'.

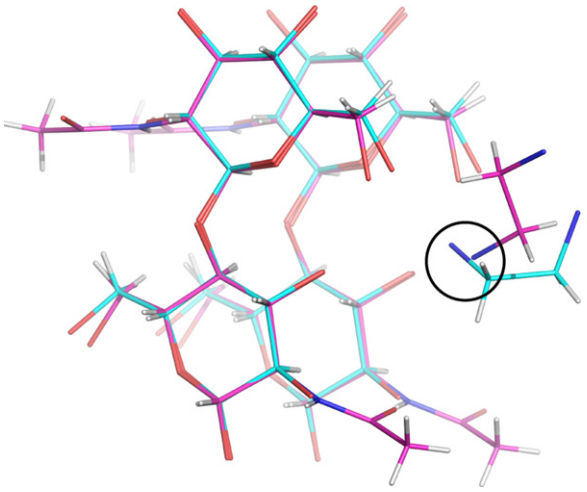

Fig. 5. Superposition of EDA cellulose I (cyan) and EDA β-chitin (purple). A nitrogen position pointed by black circle took the close position. (For interpretation of the references to color in this figure legend, the reader is referred to the web version of the article.)

These dihedral angles are similar to cellulose III_I whose ω' value is 163° and whose intramolecular hydrogen bonds from O3 is bifurcated to O5 and O6. Although *gt* conformation is considered as the major conformation by recent NMR study of α and β glucose in aqueous solution (Thibaudeau et al., 2004), the energy difference between the conformation is relatively small, and the hydrogen bonding to an amine overwhelms. Note that there would be no room for the EDA amine to hydrogen bond to O6 if the hydroxymethyl group were in *gg* conformation.

Superposition of EDA cellulose I and EDA β-chitin is shown in Fig. 5. The EDA molecules take the trans-conformation and C—C bonds are close to parallel to the chain direction in β-chitin whereas they take gauche-conformation and C—C bonds are perpendicular in cellulose I. Previously reported ab initio studies (Lee, Mhin, Cho, Lee, & Kim, 1994; Van Alsenoy, Siam, Ewbank, & Schäfer, 1986) of EDA in vacuum indicate that the gauche conformation with the most preferable lone-pare position is more stable than the trans conformation with a relative energy difference of 1.25 kcal/mol.

The short contacts between the hydrophobic planes of three structures and EDA–cellulose I complex are listed in Table 3. The distance between H2 and H3 becomes longer in the case of EDA complexes whereas shorter in the anhydrous structure and almost same in the dihydrate structure. Many potential hydrogen bonds are concentrated between O3 and neighboring O6 in EDA cellulose and especially in EDA β-chitin.

Table 3
Short inter contact between hydrophobic planes.

	H2–H3 (Å)	H2–H1 (Å)	H4–H5 (Å)
This structure	2.81	2.49	2.73
Dihydrate	2.74	2.72	2.78
Anhydrous	2.77	2.83	2.85
Cellulose-I–EDA	2.73	2.65	2.64

4. Conclusions

The crystal structure of mono-EDA β-chitin complex was determined from X-ray diffraction. The EDA molecule was clearly located in Fourier omit maps. One of the nitrogen atom is strongly bound to the primary alcohol by a hydrogen bond. The relative deposition of this nitrogen with respect to O6 and O3 was similar to that found in EDA–cellulose I. This interaction between ethylenediamine and O6 would appear to be the dominant driving interaction for complex formation with both β-chitin and cellulose.

Supplementary data

The polar coordinate diffraction data of mono-EDA β-chitin complex.

Figure of *K* vs Fc/Fcmax for refinement.

Crystallographic information file (cif) of refined structure of mono-EDA β-chitin complex by synchrotron X-ray fiber diffraction.

Observed and calculated d-spacing for unit cell determination.

Acknowledgments

Authors thank the Japan Agency for Marine-Earth Science and Technology (JAMSTEC) for collecting samples of *L. satsuma* using a remotely operated vehicle, Hyper-Dolphin. Authors thank the Japan Synchrotron Research Institute (JASRI) for the provision of beam time at BL40B2 in SPring-8.

Appendix A. Supplementary data

Supplementary data associated with this article can be found, in the online version, at http://dx.doi.org/10.1016/j.carbpol.2012.11.025.

References

Austin, P. R., Brine, C. J., Castle, J. E., & Zikakis, J. P. (1981). Chit new facets of research. *Science*, *212*, 749–753.

Blackwell, J. (1969). Structure of β-chitin or parallel chain systems of poly-β-(1→4)-*N*-acetyl-D-glucosamine. *Biopolymers*, *7*, 281–298. http://dx.doi.org/10.1002/bip.1969.360070302

Blackwell, J. (1973). The polysaccharides. In A. G. Walton, & J. Blackwell (Eds.), *Biopolymers* (pp. 464–513). New York & London: Academic Press.

Emsley, P., & Cowtan, K. (2004). Coot: Model-building tools for molecular graphics. *Acta Crystallographica Section D*, *60*, 2126–2132. http://dx.doi.org/10.1107/S0907444904019158

French, A. D., & Howley, P. D. (1989). Computer models of cellulose. In C. Schuerch, & A. Sarko (Eds.), *Cellulose and wood, chemistry and technology* (p. 159). New York: Wiley.

Gaill, F., Persson, J., Sugiyama, J., Vuong, R., & Chanzy, H. (1992). The chitin system in the tubes of deep sea hydrothermal vent worms. *Journal of Structural Biology*, *109*, 116–128. http://dx.doi.org/10.1016/1047-8477(92)90043-A

Kerwin, J. L., Whitney, D. L., & Sheikh, A. (1999). Mass spectrometric profiling of glucosamine, glucosamine polymers and their catecholamine adducts. Model reactions and cuticular hydrolysates of *Toxorhynchites amboinensis* (Culicidae) pupae. *Insect Biochemistry and Molecular Biology*, *29*, 599–607.

Kobayashi, K., Kimura, S., Togawa, E., & Wada, M. (2010). Crystal transition between hydrate and anhydrous β-chitin monitored by synchrotron X-ray fiber diffraction. *Carbohydrate Polymers*, *79*, 882–889. http://dx.doi.org/10.1016/j.carbpol.2009.10.020

Langan, P., Nishiyama, Y., & Chanzy, H. (2001). X-ray structure of mercerized cellulose II at 1 Å resolution. *Biomacromolecules*, *2*, 410–416. http://dx.doi.org/10.1021/bm.005612q

Lee, S. J., Mhin, B. J., Cho, S. J., Lee, J. Y., & Kim, K. S. (1994). Ab initio studies of the conformations of methylamine and ethylenediamine: Interaction forces affecting the structural stability. *Journal of Physical Chemistry*, *98*, 1129–1134. http://dx.doi.org/10.1021/j100055a014

Merritt, E. A., & Bacon, D. J. (1997). *Raster3D: Photorealistic molecular graphics. Macromolecular Crystallography, Part B* Academic Press. (pp. 505–524) http://www.sciencedirect.com/science/article/pii/S0076687997770289

Miserez, A., Li, Y., Waite, J. H., & Zok, F. (2007). Jumbo squid beaks: Inspiration for design of robust organic composites. *Acta Biomaterialia*, *3*, 139–149.

Miserez, A., Rubin, D., & Waite, J. H. (2010). Cross-linking chemistry of squid beak. *Journal of Biological Chemistry*, *285*, 38115–38124.

Mo, F. (1979). On the conformational variability of the N acetylglucosamine β-(1→4) dimer. Crystal and molecular structure of β-N,N'-diacetylchitobiose trihydrate. *Acta Chemica Scandinavica A*, *33*, 207–218.

Muzzarelli, R. A. A. (2011). Chitin nanostructures in living organisms. In S. N. Gupta (Ed.), *Chitin formation and diagenesis, 34* (pp. 1–34). Dordrecht: Springer.

Nishiyama, Y., Noishiki, Y., & Wada, M. (2011). X-ray structure of anhydrous β-chitin at 1 Å resolution. *Macromolecules*, *44*, 950–957. http://dx.doi.org/10.1021/ma102240r

Noishiki, Y., Kuga, S., Wada, M., Hori, K., & Nishiyama, Y. (2004). Guest selectivity in complexation of β-chitin. *Macromolecules*, *37*, 6839–6842. http://dx.doi.org/10.1021/ma0489265

Noishiki, Y., Nishiyama, Y., Wada, M., & Kuga, S. (2005). Complexation of α-chitin with aliphatic amines. *Biomacromolecules*, *6*, 2362–2364. http://dx.doi.org/10.1021/m0500446

Noishiki, Y., Nishiyama, Y., Wada, M., Okada, S., & Kuga, S. (2003). Inclusion complex of β-chitin and aliphatic amines. *Biomacromolecules*, *4*, 944–949. http://dx.doi.org/10.1021/bm034024k

Ogawa, Y., Kimura, S., & Wada, M. (2011). Electron diffraction and high-resolution imaging on highly-crystalline β-chitin microfibril. *Journal of Structural Biology*, *176*, 83–90. http://dx.doi.org/10.1016/j.jsb.2011.07.001

Parthasarathi, R., Bellesia, G., Chundawat, S. P. S., Dale, B. E., Langan, P., & Gnanakaran, S. (2011). Insights into hydrogen bonding and stacking interactions in cellulose. *Journal of Physical Chemistry A*, *115*, 14191–14202. http://dx.doi.org/10.1021/jp203620x

Rössle, M., Flot, D., Engel, J., Burghammer, M., Riekel, C., & Chanzy, H. (2003). Fast intracrystalline hydration of β-chitin revealed by combined microdrop generation and on-line synchrotron radiation microdiffraction. *Biomacromolecules*, *4*, 981–986. http://dx.doi.org/10.1021/bm0340218

Rudall, K. M. (1963). The chitin/protein complexes of insect cuticles. *Advances in Insect Physiology*, *1*, 257–313.

Saito, Y., Kumagai, H., Wada, M., & Kuga, S. (2002). Thermally reversible hydration of β-chitin. *Biomacromolecules*, *3*, 407–410. http://dx.doi.org/10.1021/bm015646d

Saito, Y., Okano, T., Gaill, F., Chanzy, H., & Putaux, J.-L. (2000). Structural data on the intra-crystalline swelling of β-chitin. *International Journal of Biological Macromolecules*, *28*, 81–88. http://dx.doi.org/10.1016/S0141-8130(00)00147-1

Sawada, D., Nishiyama, Y., Langan, P., Forsyth, V. T., Kimura, S., & Wada, M. (2012a). Direct determination of the hydrogen bonding arrangement in anhydrous β-chitin by neutron fiber diffraction. *Biomacromolecules*, *13*, 288–291. http://dx.doi.org/10.1021/bm201512t

Sawada, D., Nishiyama, Y., Langan, P., Forsyth, V. T., Kimura, S., & Wada, M. (2012b). Water in crystalline fibers of dihydrate β-chitin results in unexpected absence of intramolecular hydrogen bonding. *PLoS One*, *7*, e39376. http://dx.doi.org/10.1371/journal.pone.0039376

Schaefer, J., Kramer, K. J., Garbow, J. R., Jacob, G. S., Stejskal, E. O., Hopkins, T. L., et al. (1987). Aromatic cross-links in insect cuticle: Detection by solid-state ^{13}C and ^{15}N NMR. *Science*, *235*, 1200–1204.

Sheldrick GM. (1997). *SHELX-97, a program for the refinement of single-crystal diffraction data*. Gottingen Germany: University of Gottingen.

Sikorski, P., Hori, R., & Wada, M. (2009). Revisit of α-chitin crystal structure using high resolution X-ray diffraction data. *Biomacromolecules*, *10*, 1100–1105. http://dx.doi.org/10.1021/bm801251e

Tanner, S. F., Chanzy, H., Vincendon, M., Roux, J. C., & Gaill, F. (1990). High-resolution solid-state carbon-13 nuclear magnetic resonance study of chitin. *Macromolecules*, *23*, 3576–3583. http://dx.doi.org/10.1021/ma00217a008

Thibaudeau, C., Stenutz, R., Hertz, B., Klepach, T., Zhao, S., Wu, Q., et al. (2004). Correlated C–C and C–O bond conformations in saccharide hydroxymethyl groups: Parametrization and application of redundant $^{1}H–^{1}H$, $^{13}C–^{1}H$, and $^{13}C–^{13}C$ NMR J-couplings. *Journal of the American Chemical Society*, *126*, 15668–15685. http://dx.doi.org/10.1021/ja0306718

Van Alsenoy, C., Siam, K., Ewbank, J. D., & Schäfer, L. (1986). Ab initio studies of structural features not easily amenable to experiment. Part 49: Conformational analysis and molecular structures of ethylenediamine and aminoethanol. *Journal of Molecular Structure: Theochem*, *136*, 77–91. http://dx.doi.org/10.1016/0166-1280(86)87063-4

Wada, M., Chanzy, H., Nishiyama, Y., & Langan, P. (2004). Cellulose III_I crystal structure and hydrogen bonding by synchrotron X-ray and neutron fiber diffraction. *Macromolecules*, *37*, 8548–8555. http://dx.doi.org/10.1021/ma0485585

Wada, M., Heux, L., Nishiyama, Y., & Langan, P. (2009). The structure of the complex of cellulose I with ethylenediamine by X-ray crystallography and cross-polarization/magic angle spinning ^{13}C nuclear magnetic resonance. *Cellulose*, *16*, 943–957. http://dx.doi.org/10.1007/s10570-009-9338-5

Wada, M., Kwon, G. J., & Nishiyama, Y. (2008). Structure and thermal behavior of a cellulose I–ethylenediamine complex. *Biomacromolecules*, *9*, 2898–2904. http://dx.doi.org/10.1021/bm8006709

Yokozeki, A., & Kuchitsu, K. (1971). Structure and rotational isomerism of ethylenediamine as studied by gas electron diffraction. *Bulletin of the Chemical Society of Japan*, *44*, 2926–2930. http://dx.doi.org/10.1246/bcsj.44.2926

Yoshifuji, A., Noishiki, Y., Wada, M., Heux, L., & Kuga, S. (2006). Esterification of β-chitin via intercalation by carboxylic anhydrides. *Biomacromolecules*, *7*, 2878–2881. http://dx.doi.org/10.1021/bm060516w